Probing *n*-Spin Correlations in Optical Lattices

Chuanwei Zhang, V. W. Scarola, and S. Das Sarma Condensed Matter Theory Center, Department of Physics, University of Maryland, College Park, MD 20742

We propose a technique to measure multi-spin correlation functions of arbitrary range as determined by the ground states of spinful cold atoms in optical lattices. We show that an observation of the atomic version of the Stokes parameters, using focused lasers and microwave pulsing, can be related to n-spin correlators. We discuss the possibility of detecting not only ground state static spin correlations, but also time-dependent spin wave dynamics as a demonstrative example using our proposed technique.

PACS numbers: 03.75.Lm, 75.10.Pq, 03.75.Mn, 39.25.+k

The advent of optical lattice confinement of ultracold atomic gases [1, 2, 3, 4] opens the possibility of observing a vast array of phenomena in quantum condensed systems [5]. In particular, optical lattice systems may turn out to be the ideal tools for the analog simulation of various strongly correlated interacting lattice models (e.g. Hubbard model [2, 3], Kitaev model [6]) studied in condensed matter physics. The great advantage of optical lattices as analog simulators of strongly correlated condensed matter Hamiltonians lies in the ability of optical lattices to accurately implement the condensed matter lattice Hamiltonians without impurities, defects, lattice phonons and other complications which can obscure the observation of quantum degenerate phenomena in the solid state.

In this context optical lattices can support a variety of interacting spin models which to date have been only approximately or indirectly observed in nature or remain as rather deep but unobserved mathematical constructs. Three exciting possibilities are currently the subject of active study [5]. The first (and the most direct) envisions simulation of conventional condensed matter spin lattice models in optical lattices. Quantum magnetism arising from strong correlation leads to many-body spin ground states that can be characterized by spin order parameters. Spin order can, in some cases, show long range behavior arising from spontaneous symmetry breaking, e.g. ferromagnetism and antiferromagnetism. Such long range spin ordering phenomena are reasonably well understood in most cases. Recent work also relates conventional spin order parameters to entanglement measures which yield scaling behavior near quantum phase transitions [7, 8]. The second possibility, simulation of topological spin states, arises from the surprising fact that optical lattices can also (at least in principle) host more complicated spin models previously thought to be academic. The ground states of these models do not fall within the conventional Landau paradigm, i.e. there is no spontaneously broken symmetry, but show topological ordering and, as a result, display nontrivial short range behavior in spin correlation functions. Examples include the chiral spin liquid model [9] and the Kitaev model

[6, 10]. And finally, optical lattices are also particularly well suited to realize coherent and collective spin dynamics because dissipation can be kept to suitably low levels [11].

While optical lattices offer the possibility of realizing all three of the above examples one glaring question remains. Once a suitable spin Hamiltonian is realized, how do we observe the vast array of predicted phenomena in spin-optical lattices? To date time of flight measurements have proven to yield detailed information related to two types of important correlation functions of many-body ground states of particles trapped in optical lattices. The first, a first order correlation function (the momentum distribution), indicates ordering in one-point correlation functions [12]. The second is a second order correlation function (the noise distribution) which indicates ordering in two-point correlators [13, 14, 15, 16]. The former can, for example, detect long range phase coherence while, as we will see below, the latter is best suited to probe long range order in two-point correlation functions, e.g. the lattice spin-spin correlation function. We note that recent proposals suggest that time of flight imaging can in principle be used to extract other correlation functions [17, 18].

In this Letter we propose a technique to observe equal time n-spin correlation functions characterizing both long and short range spin ordering useful in studying all three classes of spin lattice phenomena mentioned above. Our proposal utilizes realistic experimental techniques involving focused lasers, microwave pulsing and fluorescence detection to effectively measure a general n-spin correlation function defined by: $\xi\left\{\alpha_{j_k}, k=1,...,n\right\} \equiv \langle \Psi | \prod_{k=1}^n \sigma_{j_k}^{\alpha_{j_k}} | \Psi \rangle$, where Ψ is the many-body wavefunction of the atomic ensemble, $\{j_k\}$ is a set of sites, and $\sigma_{j_k}^{\alpha_{j_k}}$ ($\alpha_{j_k}=0,1,2,3$) are Pauli spin operators at sites j_k with the notation $\sigma^0=I$, $\sigma^1=\sigma^x$, $\sigma^2=\sigma^y$, and $\sigma^3=\sigma^z$. Examples of order detectable with one, two and three-spin correlation functions are magnetization ($\langle \sigma_j^z \sigma_{j'}^z \rangle = (-1)^{j-j'}$), and chiral spin liquid order ($\langle \sigma_{j'} \times \sigma_{j''} \rangle = (-1)^{j-j'}$), and chiral spin liquid order ($\langle \sigma_{j'} \times \sigma_{j''} \rangle = 1$), to name a few.

In general our proposed technique can be used to experimentally characterize a broad class of one and two dimensional spin-lattice models of the form:

$$H(J;A) = J(t) \sum_{\{j_k\}} \left(A_{\{j_k\}} \prod_{k=1}^{M} \sigma_{j_k}^{\alpha_{j_k}} \right),$$
 (1)

where J has dimensions of energy and can vary adiabatically as a function of time, t, while the dimensionless parameters $A_{\{j_k\}}$ are kept fixed. For example, M=2 represents the usual two-body Heisenberg model. Several proposals now exist for simulating two-body Heisenberg models [5, 19]. In the following we, as an example, consider optical lattice implementations of the Heisenberg XXZ model: $H_{XXZ}(J;\Delta) = J\left[\sum_{\langle j,j'\rangle} \left(\sigma_j^x \sigma_{j'}^x + \sigma_j^y \sigma_{j'}^y\right) + \Delta \sigma_j^z \sigma_{j'}^z\right]$, where $\langle j,j'\rangle$ denotes nearest neighbors and Δ and J are model parameters that can be adjusted by, for example, varying the intensity of lattice laser beams [19].

Local Correlations in Time of Flight: We first discuss the measurement of spin-spin correlation functions by analyzing noise in time of flight from atoms confined to an optical lattice modeled by the XXZ Hamiltonian. The ground states of this and a variety of spin models can be characterized by the spin-spin correlation function between different sites. For instance, the spin-spin correlation function in a one dimensional XXZ spin chain (with J>0), shows power-law decay $\langle \sigma_j^z \sigma_{j'}^z \rangle \sim (-1)^{j-j'}/|j-j'|^{\eta}$ in the critical regime $(-1 < \Delta \le 1)$, where $\eta = 1/\left(1 - \frac{1}{\pi}\cos^{-1}\Delta\right)$. In principle this correlation function can be probed by noise in time of flight.

We argue that, in practice, short range correlations (e.g. $\eta > 1$ in the XXZ model) are difficult to detect in time of flight noise measurements. To see this note that the noise signal is proportional to [13]: G(Q(r-r')) = $\sum_{j,j'} e^{iQ\cdot \left(j'-j\right)a} \left\langle \sigma_j^z \sigma_{j'}^z \right\rangle$, where Q is the lattice wave vector which gets mapped into coordinates r and r' in time of flight on the detection screen, and a is the lattice spacing. Including normalization the noise signal is proportional to N^{-1} for systems with long range order (e.g. anti-ferromagnetic order giving $\eta = 0$ in the above XXZmodel) but shows a much weaker scaling for short range correlations. In fact the ratio between correlators in a ground state with $\eta = 0$ and $\eta > 1$ scales as N^{-1} making the state with power law correlations relatively difficult to detect in large systems. To illustrate this we compare the calculated noise correlation amplitude, G, in Fig. 1 for two cases $\eta = 0$ (solid line) and $\eta = 2$ (dashed line) with N = 200 for the 1D XXZ model. We see that the correlation amplitude for short range (powerlaw) order is extremely small in comparison to long range anti-ferromagnetic order.

The small correlation signal originates from the fact that the noise correlation method is in practice a condi-

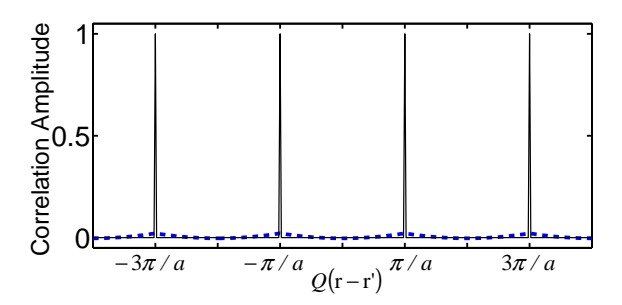


Figure 1: (color online) Noise correlation plotted as a function of wavevector of the one-dimensional XXZ model. The solid (dashed) line corresponds to a ground state with $\eta=0$, long-range ($\eta=2$, short-range) spin correlator. The amplitudes are normalized by the maximum for the antiferromagnetic order giving $\eta=0$.

tional probability measuring collective properties of the whole system, while short range spin correlations describe local properties and are therefore best detected via local operations. In the following we propose a local probe technique to measure local correlations thus providing an experimental scheme which compliments the time of flight-noise correlation technique, best suited for detecting long range order.

Detecting n-spin Correlation with Local Probes: We find that general n-spin correlators, ξ { α_{j_k} , k=1,...,n}, can be related to the Stokes parameters broadly defined in terms of the local reduced density matrix $\rho = \text{Tr}_{\{j_k,k=1,...,n\}} |\Psi\rangle \langle \Psi|$ on sites $\{j_k,k=1,...,n\}$, where the trace is taken on all sites except the set $\{j_k\}$. The Stokes parameters for the density matrix ρ are $S_{\alpha_{j_1}....\alpha_{j_n}} = \text{Tr}\left(\rho\prod_{k=1}^n\sigma_{j_k}^{\alpha_{j_k}}\right)$ leading to the decomposition $\rho = 2^{-n}\sum_{\alpha_{j_1},...,\alpha_{j_n}=0}^3 \left[S_{\alpha_{j_1}....\alpha_{j_n}}\prod_{k=1}^n\sigma_{j_k}^{\alpha_{j_k}}\right]$. Using the theory of quantum state tomography [20], we find the n-spin correlators ξ { α_{j_k} , k=1,...,n} = $\prod_{k=1}^n \left(P\left\{\left|\phi_{\alpha_{j_k}}\right.\right\rangle\right\} \pm P\left\{\left|\phi_{\alpha_{j_k}}^{\perp}\right.\right\rangle\right\}$, where the plus (minus) sign indicates a 0 (non-zero) index and $\left\{\left|\phi_{\alpha_{j_k}}\right.\right\rangle, \left|\phi_{\alpha_{j_k}}^{\perp}\right.\right\rangle$ denote the measurement basis for the atom at j_k . We define the measurement basis to be: $|\phi_1\rangle = (|\downarrow\rangle + |\uparrow\rangle)/\sqrt{2}, \ |\phi_2^{\perp}\rangle = (|\downarrow\rangle - |\uparrow\rangle)/\sqrt{2}, \ |\phi_3\rangle = |\downarrow\rangle, \ |\phi_3^{\perp}\rangle = |\uparrow\rangle$. Finally, $P\left\{\left|\phi_{\alpha_{j_k}}\right.\right\rangle$ is the probability of finding an atom in the state $|\phi_{\alpha_{j_k}}\rangle$.

The expansion of the product defining ξ then yields a quantity central to our proposal:

$$\xi \left\{ \alpha_{j_k}, k = 1, ..., n \right\} = \sum_{l=1}^{n} (-1)^l P_l, \tag{2}$$

where P_l is the probability of finding l sites in the states $|\phi_{j_k}^{\perp}\rangle$ and n-l sites in $|\phi_{j_k}\rangle$. Eq. (2) shows that the n-spin correlation function can be written in terms of ex-

perimental observables. We can now write a specific example of the two-spin correlation function (discussed in the previous section) in terms of observables: $\xi\left\{3,3\right\}=P_{|\downarrow\rangle_{j_1}|\downarrow\rangle_{j_2}}+P_{|\uparrow\rangle_{j_1}|\uparrow\rangle_{j_2}}-\left(P_{|\downarrow\rangle_{j_1}|\uparrow\rangle_{j_2}}+P_{|\uparrow\rangle_{j_1}|\downarrow\rangle_{j_2}}\right).$ In the following section we discuss a specific experimental procedure designed to extract precisely this quantity using local probes of cold atoms confined to optical lattices.

Proposed Experimental Procedure: We now describe and critically analyze an experimental procedure designed to find the probabilities, P_l , from a single two dimensional (xy plane) optical lattice with the assistance of applied microwave pulses and focused lasers. Here the atomic dynamics in the z direction are frozen out by high frequency optical traps [21]. We consider a setup in which the overall prefactor, i.e. the spin coupling strength J(t), in Eq. (1) can be controlled by varying the lattice depth. To illustrate our technique we consider, without loss of generality, a specific realization: ^{87}Rb atoms with two hyperfine ground states chosen as the spin of each atom. In the Mott insulator regime with one atom per lattice site, various spin Hamiltonians may be implemented using spin-dependent lattice potentials in the super-exchange limit [19]. Our proposed experimental procedure will build on such spin systems, although it can be generalized to other implementations where H is generated by other means.

In step (i) we start with a many-body spin state and turn off the spin-spin interactions generated by super exchange between lattice sites. We achieve this by ramping up the lattice depth to $\sim 50 E_R$ adiabatically with respect to the band splitting. The time scale for the spin-spin interactions ($\sim \hbar/J$) becomes much longer than the time taken to perform the steps that follow. The ramp up preserves the highly correlated spin state by merely changing the overall energy scale. The following steps are quickly performed on this "frozen" many-body spin state.

In step (ii) a combination of microwave pulses and focused lasers [22] is used to transfer target atoms A at site(s) j_k to a suitable measurement basis $\{|\phi_{j_k}\rangle, |\phi_{j_k}^{\perp}\rangle\}$ from initial states $\{|\downarrow\rangle_{j_k}, |\uparrow\rangle_{j_k}\}$, without affecting nontarget atoms B at other sites. The spin states we consider here are $|\downarrow\rangle\equiv|F=1,m_F=-1\rangle$ and $|\uparrow\rangle\equiv|F=2,m_F=-2\rangle$. With a properly chosen intensity, the focused laser induces shifts of the hyperfine splitting between states $|\downarrow\rangle$ and $|\uparrow\rangle$ and the differences of the shifts between atoms A and B can be larger than $\delta=74E_r$, where $E_r=h^2/2m\lambda^2$ is the photon recoil energy and λ is the wavelength of the optical lattice. The adiabatic condition yields a $35\mu s$ ramp up time of the focused laser that corresponds to a 10^{-4} probability for excitation to higher bands.

We then change the measurement basis by applying a microwave $\pi/2$ pulse that drives a suitable rotation to target atoms A. The microwave is resonant with the hyperfine splitting of the target atoms A, but has a detuning

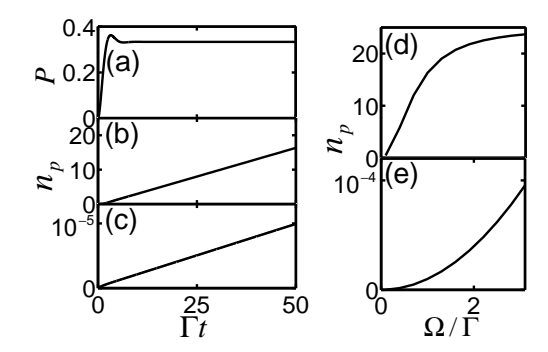


Figure 2: (a) Time evolution of the probability for the target atoms A to be in the excited state $|3\rangle$. (b) and (c) plot the number of scattering photons versus time for atoms A and B, respectively. (d) and (e) plot the same but versus the Rabi frequency of the resonant laser for atoms A and B, respectively. Γ is the spontaneous decay rate.

larger than δ for non-target atoms B. Consider a pulse with Rabi frequency $\Omega(t) = \Omega_0 \exp\left(-\omega_0^2 t^2\right) \left(-t_f \le t \le t_f\right)$ and parameters $\omega_0 = 14.8 E_r/\hbar$, $\Omega_0 = 13.1 E_r/\hbar$ and $t_f = 5/\omega_0$. The pulse transfers the measurement basis of the target atoms A in $16.9 \mu s$, while the change in the quantum state of non-target atoms is found to be below 3×10^{-4} by numerically integrating the Rabi equation that describes the coupling between two spin states by the microwave pulse. The focused lasers are adiabatically turned off after the microwave pulse. During the whole process, the probability for spontaneous scattering of one photon from target atoms inside the focused laser is estimated to be around 2×10^{-4} .

In step (iii) we transfer all atoms to the $|F=1\rangle$ hyperfine level to avoid stray signal in the detection step (iv). We apply two π microwave pulses to transfer all atoms at $|\downarrow\rangle$ to $|2\rangle \equiv |F=1, m_F=1\rangle$ and then another π microwave pulse to transfer all atoms at $|\uparrow\rangle$ to $|\downarrow\rangle$. The π microwave pulse can be implemented within 12.5 μs for a microwave Rabi frequency $\Omega=2\pi\times 40KHz$.

In step (iv) we transfer target atoms A at j_k from $|\downarrow\rangle$ back to $|\uparrow\rangle$ with the assistance of the focused lasers, and then apply a detection laser resonant with $|\uparrow\rangle \rightarrow |3\rangle \equiv |5^2P_{3/2}:F=3,m=-3\rangle$ to detect the probability of finding target atoms at $|\uparrow\rangle$ (corresponding to the basis state $|\phi_{j_k}^{\perp}\rangle$ because we transferred atoms to the measurement basis in step (ii)). The fluorescence signal (the number of scattered photons) is from one of the n+1 quantized levels, where the l-th level (l=0,...,n) corresponds to states with l sites on state $|\phi_{j_k}^{\perp}\rangle$. By repeating the whole process many times, we obtain the probability distribution P_l , and thus the spin correlation function ξ { $\alpha_{j_k}, k=1,...,n$ } via Eq. (2).

The scattering photons come mostly from the target atoms A at state $|\uparrow\rangle$. Signal from atoms at any $|F=1\rangle$ state is suppressed because of the large hyperfine splitting $(\nu \approx 2\pi \times 6.8 GHz)$ between $|F=1\rangle$ and $|F=2\rangle$ states.

The dynamics of photon scattering is described by the optical Bloch equation, from which we can numerically calculate the number of scattering photons $n_p(t)$ for both target and non-target atoms. From Fig. 2 we see that the probability to find target atoms at the excited state $|3\rangle$ increases initially and reaches a saturation value. The number of scattering photons reaches a large number (\sim 20) in a short period $1.3\mu s$ for atoms A (Fig. 2(b)), but the scattering number for B atoms is small ($\sim 10^{-5}$) (Fig. 2(c)). The scattering photons from the non-target atoms B can therefore be neglected. In Fig. 2(d) and (e), we see that for a wide range of Rabi frequencies, the scattering photon number for the non-target atoms B is suppressed to undetectable levels, below 10^{-4} .

Unlike the noise correlation method, the accuracy of our detection scheme does not scale with the number of total atoms, but is determined only by manipulation errors in the above steps. We estimate that n-spin correlations can be probed at an accuracy $\sim n \times 10^{-2}$, which is sufficient to measure both long and short range spin correlation functions. We have proposed a powerful technique for investigating strongly-correlated spin models in optical lattices and now consider one of its several possible applications.

Spin Wave Dynamics: Our technique can be used to investigate time-dependence of correlation functions. In the following, we show how our scheme can be used to engineer and probe spin wave dynamics in a straightforward example, the Heisenberg XX model realized in optical lattices with a slightly different implementation scheme than the one discussed in the previous section. Consider a Mott insulator state with one boson per lattice site prepared in the state $|0\rangle \equiv |F=1, m_F=-1\rangle$ in a single two dimensional (xy) plane. By varying the trap parameters or with a Feshbach resonance, the interaction between atoms can be tuned to the hard-core limit. With a large optical lattice depth in the y direction, the system becomes a series of one dimensional tubes with dynamics described by the Bose-Hubbard Hamiltonian: $-\chi(t)\sum_{j}\left(a_{j}^{\dagger}a_{j+1}+a_{j+1}^{\dagger}a_{j}\right)$. This Hamiltonian maps onto the XX spin model, $H_{XXZ}(-2\chi; \Delta=0)$, with the Holstein-Primakoff transformation. This spin model can be solved exactly offering a testbed for spin wave dynam-

We now study the time dependent behavior of the XX model using our proposed scheme. In the Heisenberg picture, the time evolution of the annihilation operator can be written as: $a_j(t) = \sum_{j'} a_{j'}(0) i^{j'-j} J_{j'-j}(\alpha)$, where $J_{j'-j}(\alpha)$ is the Bessel function of the interaction parameter $\alpha(t) = 2 \int_0^t \chi(t') dt'$. To observe spin wave dynamics, we first flip the spin at one site from \uparrow to \downarrow , which, in the bosonic degrees of freedom, corresponds to removing an atom at that site. Because of the spin-spin interactions, initial ferromagnetic order gives way to a re-orientation of spins at neighboring sites which propagates along the

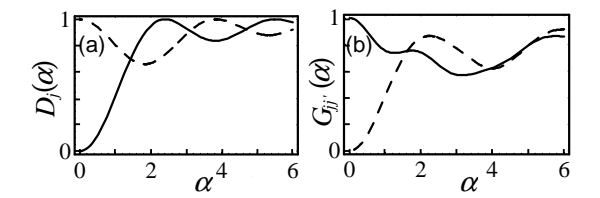


Figure 3: Plots of site occupation probability (a) and density-density correlation (b) with respect to scaled spin interaction parameter $\alpha \propto$ time for N=30 and: j=0 ((a)-dashed line); j=1 ((a)-solid line); j=0, j'=3 ((b)-dashed line); and j=2, j'=3 ((b)-solid line).

spin chain in the form of spin waves. This corresponds to a time dependent oscillation of atom number at each site. Therefore, spin wave dynamics can be studied in one and two point spin correlation functions by detecting the oscillation of the occupation probability at certain sites and the density-density correlator between different sites, respectively.

Single atom removal at specific sites can be accomplished with the assistance of focused lasers. With a combination of microwave radiation and focused lasers, we can selectively transfer an atom at a certain site from the state $|0\rangle$ to the state $|1\rangle \equiv |F=2, m_F=-2\rangle$. A laser resonant with the transition $|1\rangle \rightarrow |3\rangle$ is then applied to remove an atom at that site. Following an analysis similar to the one above, we see that the impact on other atoms can be neglected. To observe fast dynamics of spin wave propagation, we may adiabatically ramp down the optical lattice depth (and therefore increase χ) from the initial depth $V_0 = 50E_r$ to a final depth $13E_r$, with a hold time, t_{hold} , to let the spin wave propagate. Finally, the lattice depth is adiabatically ramped back up to V_0 for measurement. The time dependence of the lattice depth in the ramping down process is chosen to be $V(t) = V_0 / \left(1 + 4\sqrt{2P_{\rm exe}V_0/E_r}\omega_r t\right)$, where $P_{\rm exe}$ is the probability of making an excitation to higher bands and $\omega_r = E_r/\hbar$. For $P_{\text{exe}} = 4 \times 10^{-4}$, we find the interaction parameter to be $\alpha(t_{\text{hold}}) =$ $0.0146 + 0.0228\omega_r t_{\mathrm{hold}}$, with the tunneling parameter: $\chi\left(t\right) = \left(4/\sqrt{\pi}\right) E_r^{1/4} V^{3/4}\left(t\right) \exp\left(-2\sqrt{V\left(t\right)/E_r}\right)$.

Two physical quantities that can be measured in experiments are the single atom occupation probability $D_{j}(\alpha) = \langle \varphi | a_{j}^{+} a_{j} | \varphi \rangle = \sum_{l \neq \eta} J_{l-j}^{2}(\alpha)$ at the site j, and the density-density correlator $G_{jj'}(\alpha) = \langle \varphi | a_{j}^{+} a_{j} a_{j'}^{+} a_{j'} | \varphi \rangle = \sum_{l \neq \eta, \gamma \neq \eta} J_{l-j}^{2}(\alpha) J_{\gamma-j'}^{2}(\alpha) - \sum_{l \neq \eta} (J_{l-j}^{2}(\alpha) J_{l-j'}^{2}(\alpha) + J_{l-j}(\alpha) J_{\eta-j'}(\alpha) J_{\eta-j'}(\alpha) J_{l-j'}(\alpha))$ between sites j and j', where φ is the initial wavefunction with one removed atom at site η . The former is related to the local transverse magnetization through $\langle \varphi | s_{z}^{z}(\alpha) | \varphi \rangle = D_{j}(\alpha) - 1/2$, and the latter is re-

lated to the spin-spin correlator via $G_{jj'}(\alpha) = \langle \varphi | s_j^z(\alpha) s_{j'}^z(\alpha) | \varphi \rangle + (D_j(\alpha) + D_{j'}(\alpha))/2 + 1/4$. In Fig. 3, we plot $D_j(\alpha)$ and $G_{jj'}(\alpha)$ with respect to the interaction parameters α (which scales linearly with holding time). We see different oscillation behavior at different sites, indicating the propagation of a spin wave along the one dimensional optical lattice.

To probe the single site occupation probability $D_j(\alpha)$, we use a focused laser and a microwave pulse to transfer the atom at site j to $|1\rangle$. A laser resonant with the transition $|1\rangle \rightarrow |3\rangle$ is again applied to detect the probability to have an atom at $|1\rangle$, which is exactly the occupation probability $D_j(\alpha)$. To detect $G_{jj'}(\alpha)$, we transfer atoms at both sites j and j' to the state $|1\rangle$ and use the same resonant laser to detect the joint probability for atoms at $|1\rangle$. The fluorescence signal has three levels, which correspond to both atoms $G_{jj'}(\alpha)$, one atom $D_j(t) + D_{j'}(t)$, and no atoms at state $|1\rangle$. A combination of these measurement results gives the spin-spin correlator $\langle \varphi | s_z^z(\alpha) s_{j'}^z(\alpha) | \varphi \rangle$.

We find that a relation between general spin correlation functions and observable state occupation probabilities in optical lattices allows for quantitative measurements of a variety of spin correlators with the help of local probes, specifically focused lasers and microwave pulsing. Applications to a broad class of spin physics including topological phases of matter [6, 10] realized in spin-optical lattices are also possible with our proposed technique.

This work is supported by ARO-DTO, ARO-LPS, and LPS-NSA.

- [1] P. S. Jessen *et al.*, Phys. Rev. Lett. **69**, 49 (1992).
- D. Jaksch et al., Phys. Rev. Lett. 81, 3108 (1998).
- [3] M. Greiner et al., Nature (London) 415, 39 (2002).
- [4] B. Paredes et al., Nature (London) 429, 277 (2004).
- [5] M. Lewenstein, et al., arXiv:cond-mat/0606771.
- A. Kitaev, Ann. Phys. 321, 2 (2006).
- [7] A. Osterloh, et al., Nature 416, 608 (2002).
- [8] T. Poscilde, et al., Phys. Rev. Lett. 93, 167203 (2004); ibid. 94, 147208 (2005).
- [9] X. G. Wen, et al., Phys. Rev. B 39, 11413 (1989).
- [10] C. Zhang, et al., arXiv:quant-ph/0609101.
- [11] A. Widera, et al., Phys. Rev. Lett. 95, 190405 (2005); F. Gerbier, et al., Phys. Rev. A 73, 041602(R) (2006).
- [12] W. Ketterle, et al., arXiv:cond-mat/9904034.
- [13] E. Altman, et al., Phys. Rev. A 70, 013603 (2004).
- [14] M. Greiner, et al., Phys. Rev. Lett. 92, 150405 (2004).
- [15] S. Foelling, et al., Nature **434**, 481 (2005).
- [16] I.B. Spielman, et al., arXiv:cond-mat/0606216.
- [17] L.-M. Duan, Phys. Rev. Lett. 96, 103201 (2006).
- [18] Q. Niu et al., Phys. Rev. A 73, 053604 (2006).
- [19] L.-M. Duan, et al., Phys. Rev. Lett. 91, 090402 (2003).
- [20] J.B. Altepeter, et al., in Quantum State Estimation, Ed. by M.G.A. Paris and J. Rehacek, Springer Berlin (2004).
- [21] T.P. Meyrath, et al., Phys. Rev. A 71, 041604(R) (2005).
- [22] C. Zhang, et al., Phys. Rev. A 74, 042316 (2006).